

## Introduction

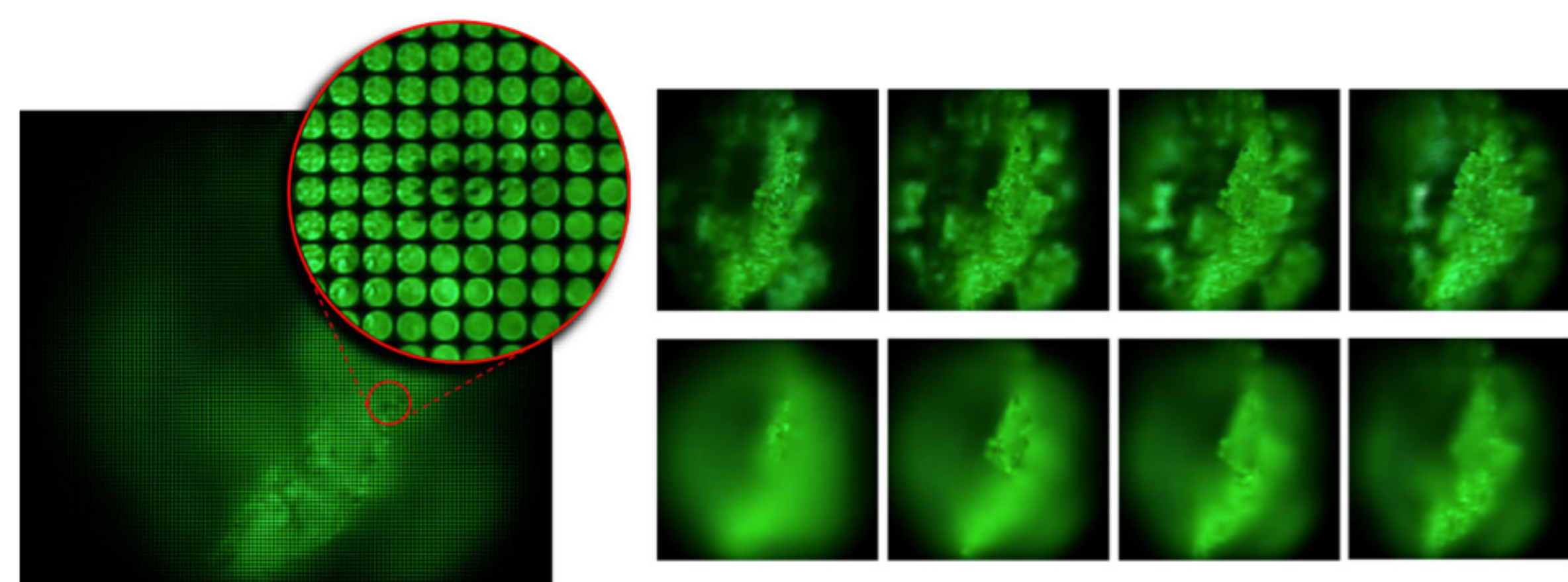


Fig. 1 – At the left is a light field captured by photographing a speck of fluorescent crayon wax through a microscope objective and micro lens array. The objective magnification is 16 $\times$ , and the field of view is 1.3mm wide. The image consists of 1702 sub-images, one per micro lens, each depicting a different part of the specimen. An individual sub-image contains 202 pixels, each representing a different point on the objective lens and hence a unique direction of view. Extracting one pixel from each sub-image produces perspective views of the specimen, a sequence of which is shown at top-right. Alternatively, by summing the pixels in each sub-image, we can produce orthographic views with a shallow depth of field, like an ordinary microscope but of lower spatial resolution. Shearing the light field before summing, we can focus at different depths, as shown in the sequence at bottom-right. These images were computed in real-time on a PC. [1]

## Theory

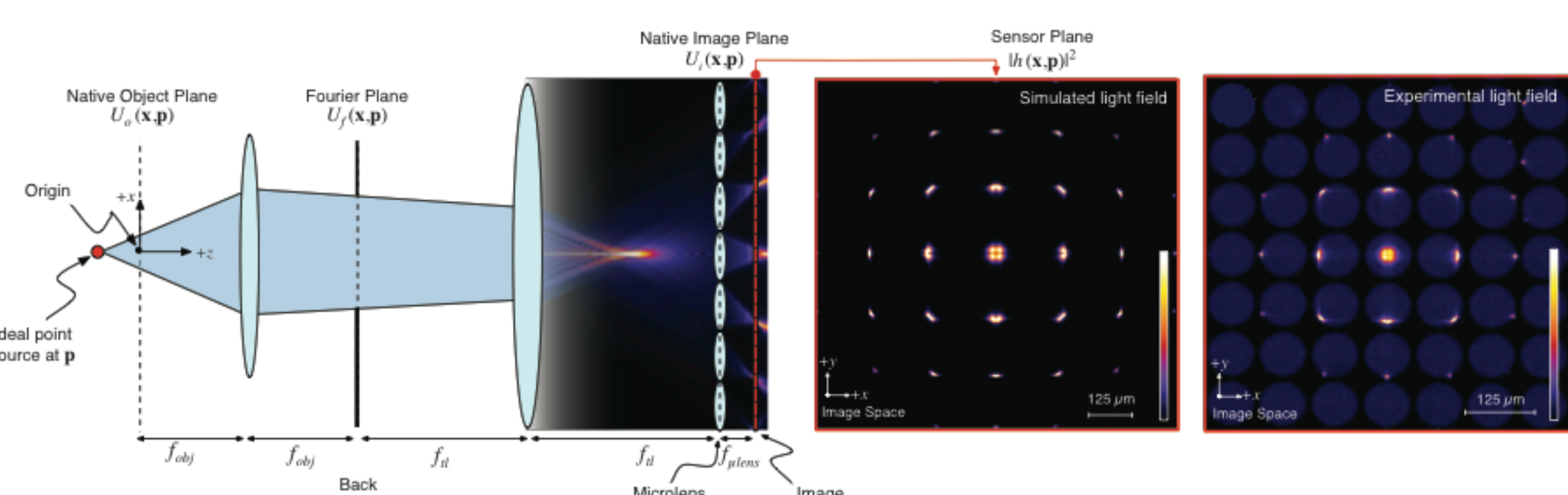


Fig. 2 – Schematic of wave optics model based on the optical path of an LFM. Here, at the native image plane the micro lens array is modeled as a tiled phase mask operating on this wavefront, which then propagates onto the camera sensor. The simulated light field using this model agrees well with an experimentally produced light field. [2]

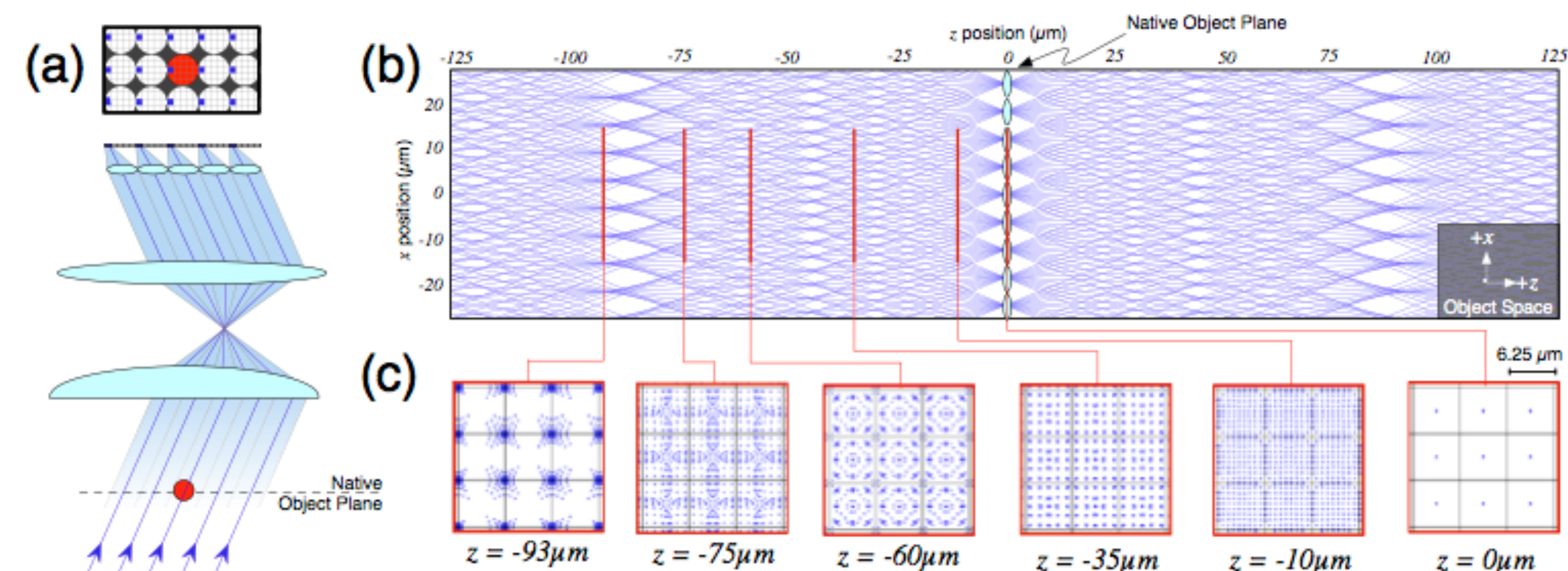


Fig. 3 – (a) A bundle of chief rays captured by the same pixel position relative to each lenslet (blue pixels) provides one of the many angular views necessary for 3-D deconvolution. (b) When lenslet chief rays passing through every pixel in the light field are simultaneously projected back into the object volume they cross a diversity of x positions. The only place where there is no diversity is at  $z=0\mu\text{m}$ . (c) The distribution of the lenslet chief rays in  $xy$  cross-sections of the object volume changes at different distances from the native object plane. [2]

A micro lens array is critical to the operation of the LFM. Here, micro lens array and objective are paired with respect to  $f/\#$ . The numerical aperture (NA) is chosen to maximize resolution and magnification (M) of the objective is chosen to optimize the lateral field of view. Other important parameters include the number of resolvable spots in each micro lens (S) and the pitch (p). The combination of micro lens array and objective determine the overall lateral and axial resolutions of reconstructed light fields.

Design Criterion	Physical Relation	LFM
$R_{obj}$	$\frac{0.47\lambda n}{NA}$	9.57 $\mu\text{m}$
Resolvable Spots (S)	$p/R_{obj}$	13.6
Lateral Resolution	$p/M$	6.5 $\mu\text{m}$
Axial Resolution	$\frac{\lambda n}{(NA)^2}$	2.04 $\mu\text{m}$
Focal Plane Resolution	$\frac{(2+S)\lambda n}{2(NA)^2}$	16 $\mu\text{m}$
Depth of View	$\frac{(2+S^2)\lambda n}{2(NA)^2}$	190 $\mu\text{m}$

Table 1 – Design criteria of LFM are listed with respective physical relations derived with varied consideration to wave and to geometrical optics [3]. LFM refers to our system and its given performance with a 20 $\times$ /0.5 objective and micro lens with a pitch  $p=130\mu\text{m}$ . Here, the wavelength of light is 509nm chosen to match the emission of GFP. The index of refraction  $n=1$  for air.

## Results

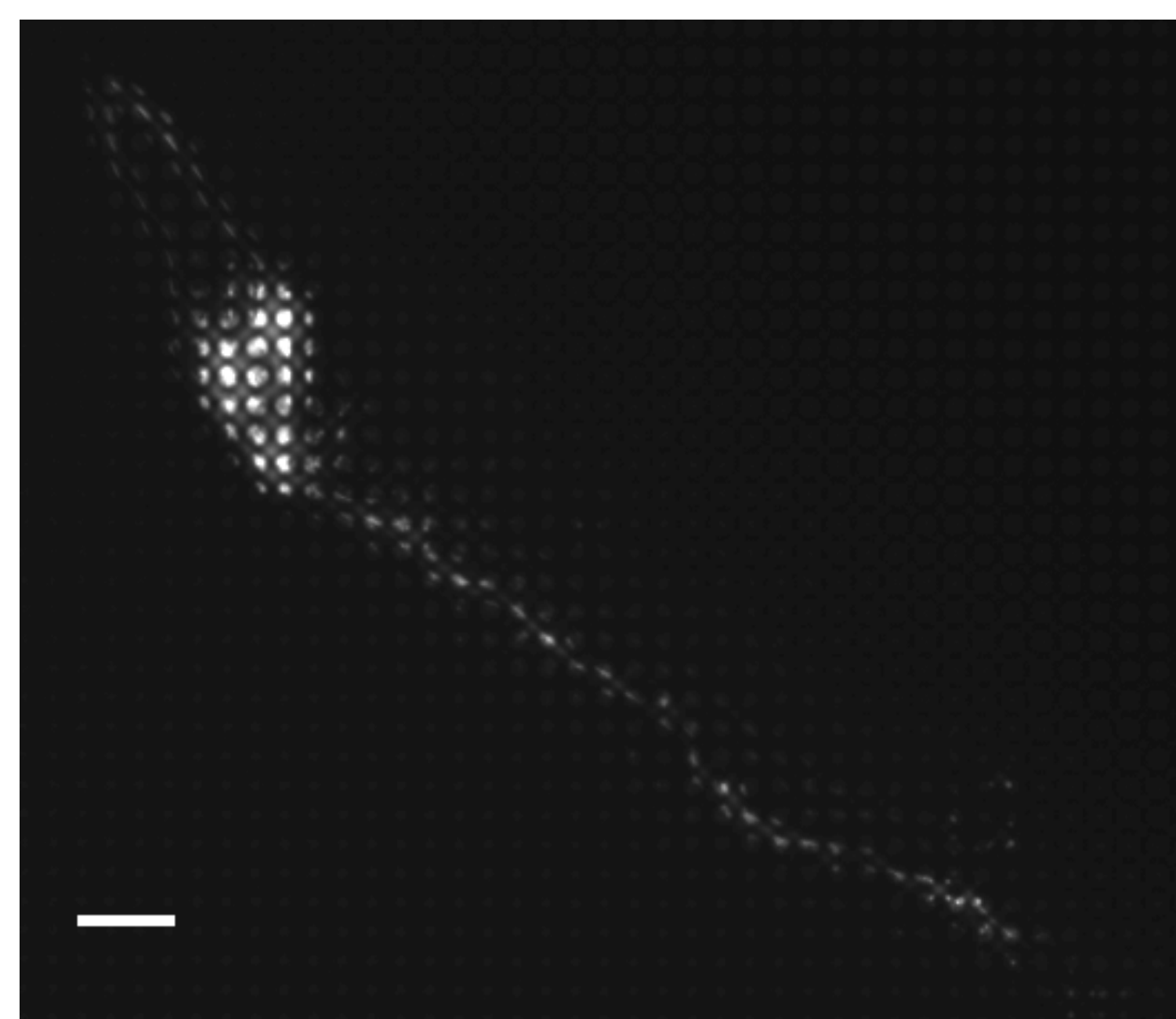


Fig. 4 – Captured light field of *C. elegans* using LFM. Lateral field of view is 395 $\mu\text{m} \times 335\mu\text{m}$ . Scale bar is 33 $\mu\text{m}$ .

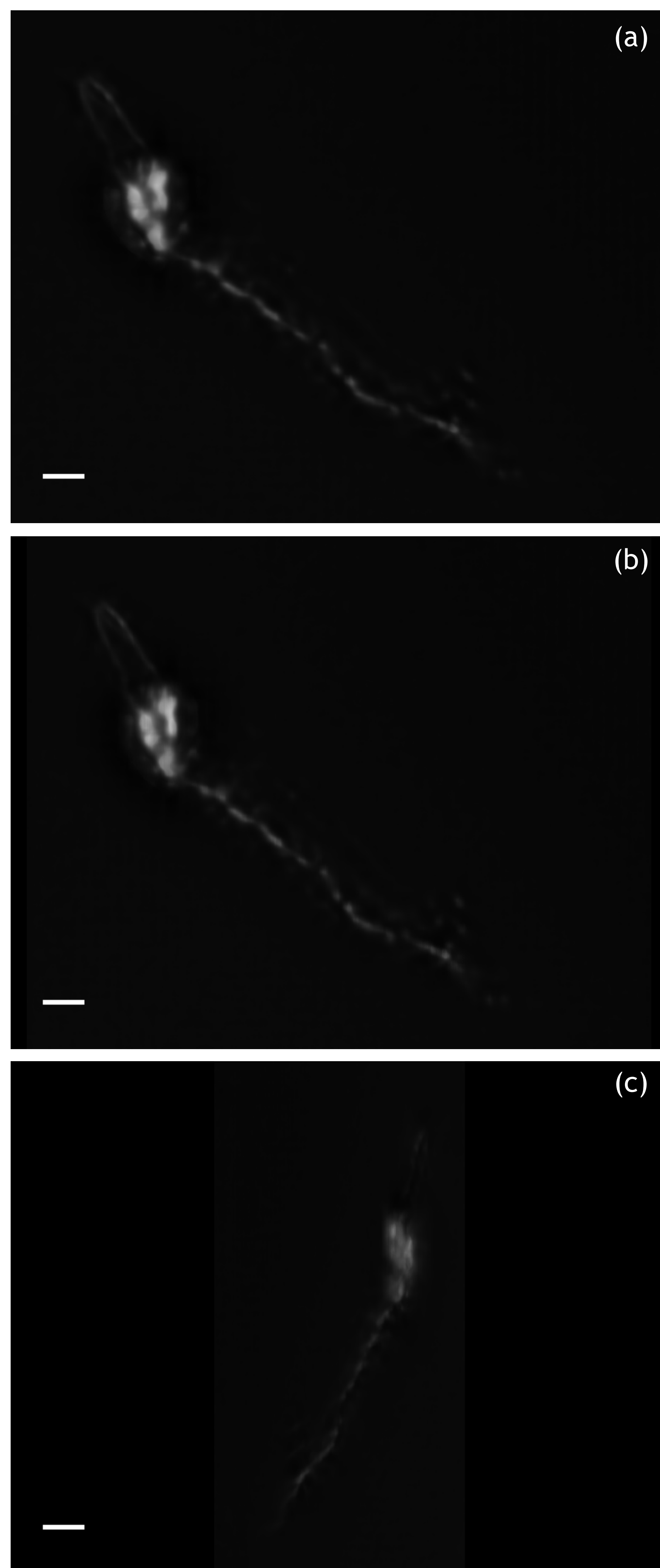


Fig. 5 – Eleven focal slices of forty that result from the volume reconstruction of the light field shown in Fig. 6. Scale bar is 33 $\mu\text{m}$ . Respective focal planes are: a)  $z=42.75\mu\text{m}$ , b)  $z=38.25\mu\text{m}$ , c)  $z=31.5\mu\text{m}$ , d)  $z=15.75\mu\text{m}$ , e)  $z=6.75\mu\text{m}$ , f)  $z=0\mu\text{m}$ , g)  $z=-9\mu\text{m}$ , h)  $z=-15.75\mu\text{m}$ , i)  $z=-24.75\mu\text{m}$ , j)  $z=-31.5\mu\text{m}$ , and k)  $z=-40.5\mu\text{m}$ .

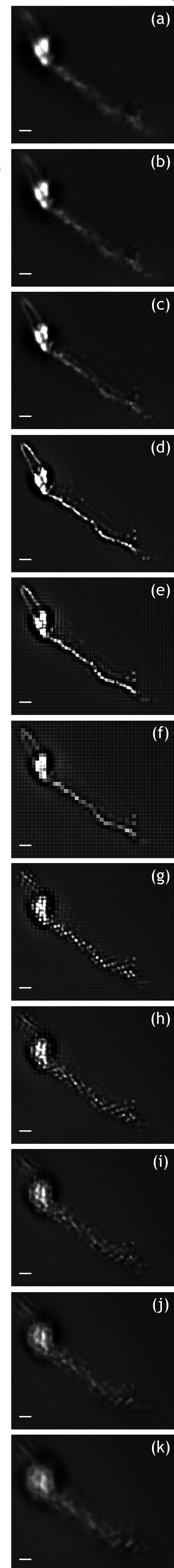
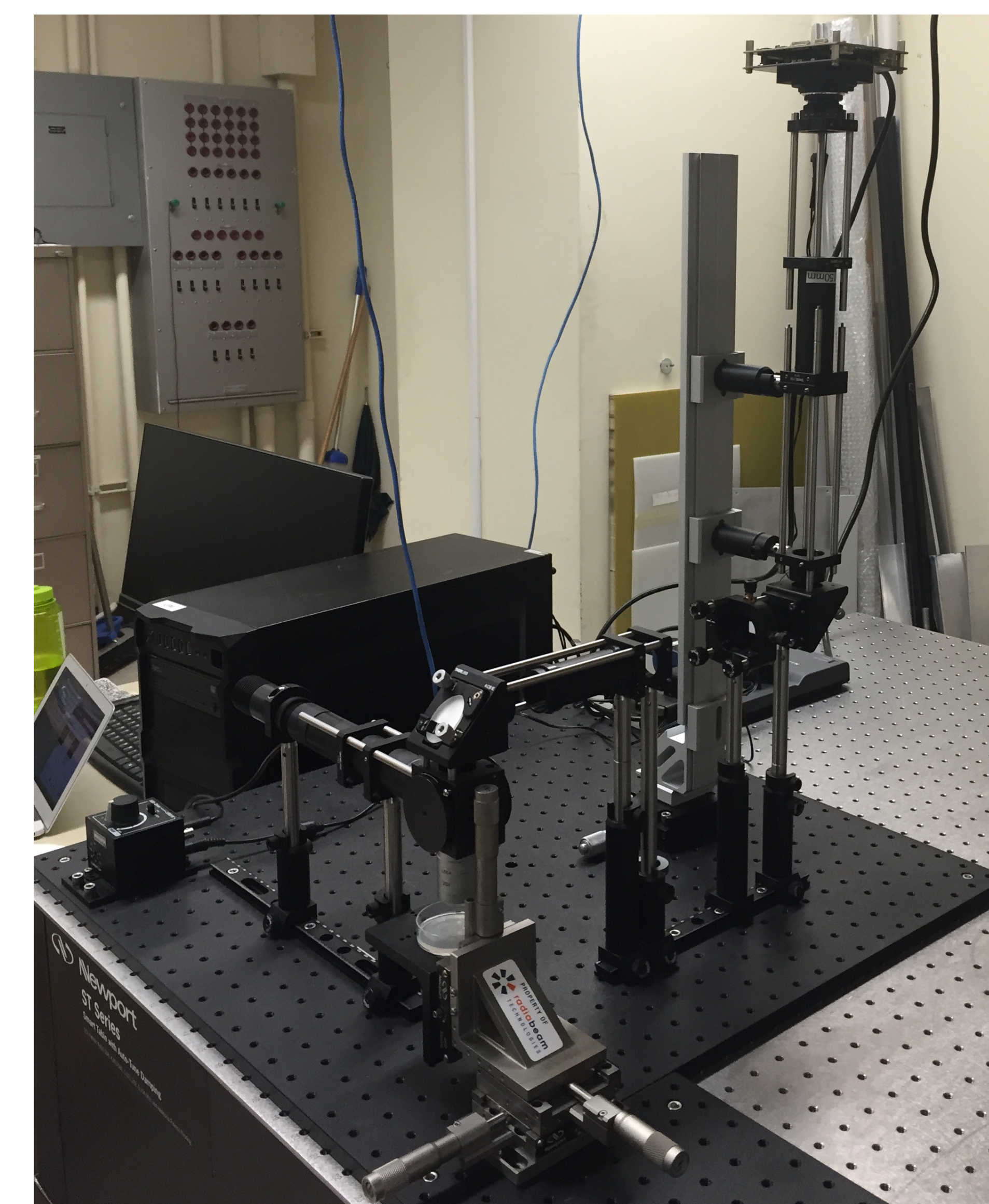


Fig. 6 – Different perspectives of mean value intensity 3D-projection of 33 focal slices reconstructed from uncropped light field shown in Fig. 6. Field of view is 520 $\mu\text{m} \times 405\mu\text{m} \times 90\mu\text{m}$ . Scale bar is 50 $\mu\text{m}$ . Angles (in degrees) of perspectives are a) 0, b) 30, and c) 120.

## Methods



Images are acquired using Hamamatsu Flash 4.0 board level camera attached to epifluorescence microscope with micro lens array placed at intermediate image plane. Reconstruction of focal stacks from light fields are carried out with open source software<sup>3</sup>. Image rendering and further post-processing is performed with open source software Fiji.



Fig. 8 – Micro lens array on a five-axis kinematic mount.

Fig. 7 – Light field microscope utilized to image *C. elegans*. Here, an objective of 20X 0.5NA is used in conjunction with a 130 $\mu\text{m}$  pitch  $f/20$  micro lens array. A 1:1.5 relay system is used in order to utilize the entire camera detector plate resulting in a maximum lateral field of view of 665 $\mu\text{m} \times 665\mu\text{m}$ .

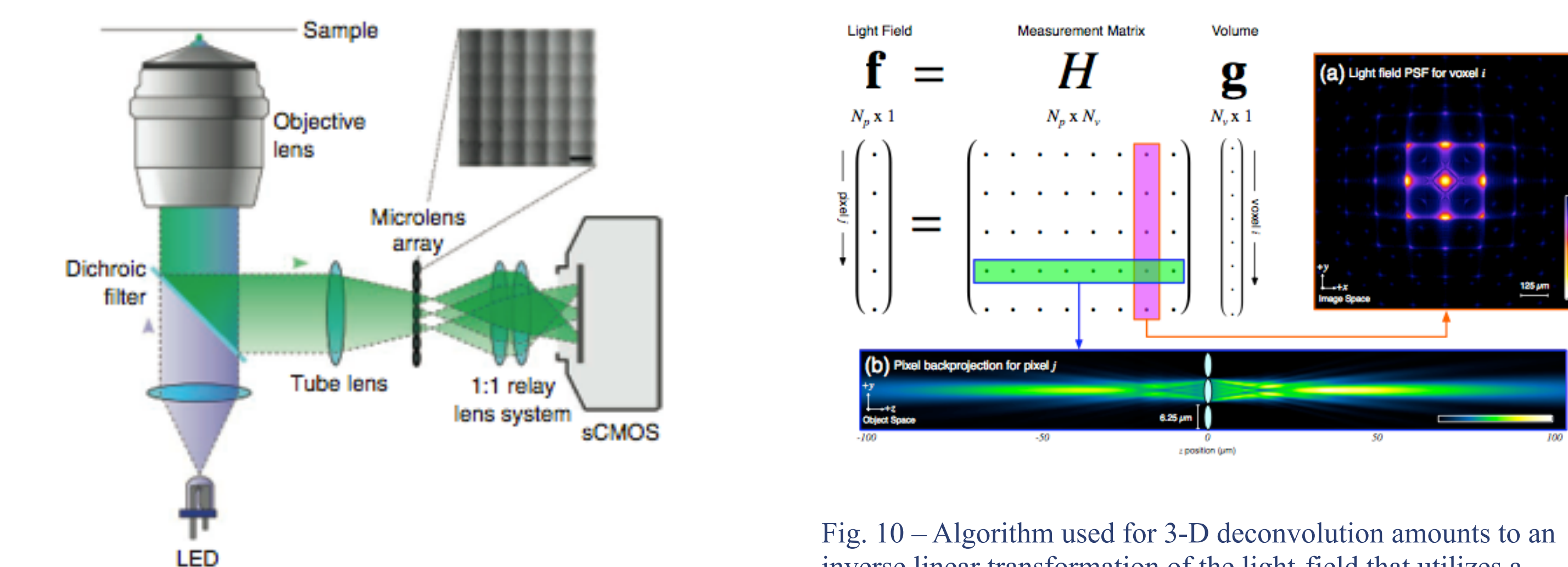


Fig. 9 – Conceptual schematic of LFM. It is an epifluorescence microscope with a micro lens array placed at the intermediate image plane. [3]

Fig. 10 – Algorithm used for 3-D deconvolution amounts to an inverse linear transformation of the light-field that utilizes a computed point-spread function (PSF) (a) to determine matrix  $H$ . (b) The pixel back projection contained in row  $j$  of the measurement matrix shows the contribution of each voxel in the volume on a single pixel  $j$  in the light field. [3]

## Future Directions

To further improve the light field microscope at imaging *C. elegans*, custom micro lens arrays can be designed to match high NA objectives. Larger micro lens arrays provide axial resolution at the cost of lateral resolution. Powerful commercially available GPUs can significantly reduce post-processing for large-scale image processing. The next phase of data acquisition will be 3D videos with optimal temporal resolution with regard to light field information. This will allow for acquisition of real-time neural dynamics in conjunction with behavioral activity.

## References

- Levoy, M., et al. "Light Field Microscopy." *ACM Transactions on Graphics* **25.3** 924 (2006).
- Broxton, M. et al. "Wave optics theory and 3-D deconvolution for the light field microscope." *Opt. Express* **21**, 25418-25439 (2013).
- Prevedel R., et al. "Simultaneous whole-animal 3D-imaging of neuronal activity using light field microscopy." *Nature Methods* **11.7** (2014).

## Acknowledgements

Special thanks to Michelle Kao, Shirley Cheng, and Karen Jiang for countless sample preparations, Paul Chin for aiding the design of the microscope illumination, Blake Madruga for consultation with regards to optics, Vilmey Filho for assistance in streamlining open source code for volume reconstruction, and to the National Science Foundation (NSF) for funding this research.